Supplementary data for

Facilitated hyperpolarization signaling in vascular smooth muscle overexpressing TRIC-A channels*

Shengchen Tao[1#], Daiju Yamazaki[1,2#], Shinji Komazaki[3], Chengzhu Zhao[1], Tsunaki Iida[1], Sho Kakizawa[1], Yuji Imaizumi[4], and Hiroshi Takeshima[1,2,5]

[1]Graduate School of Pharmaceutical Sciences and [2]Center for the Promotion of Interdisciplinary Education and Research, Kyoto University, Kyoto 606-8501, Japan.

[3]Saitama Medical University, Saitama 350-0495, Japan.

[4]Graduate School of Pharmaceutical Sciences, Nagoya City University, Aichi 467-8603, Japan.

*****Running title: *Tric-a*-overexpressing vascular smooth muscle

[#]Both authors contributed equally to this work.

[5]Corresponding Author: Hiroshi Takeshima, Department of Biological Chemistry, Graduate School of Pharmaceutical Sciences, Kyoto University, Kyoto 606-8501, Japan.

E-mail: takeshim@pharm.kyoto-u.ac.jp; Tel: +81-75-753-4572; Fax: +81-75-753-4605

SUPPLEMENTARY FIGURE LEGENDS

SUPPLEMENTARY FIGURE S1. **Postnatal growth, *Tric-a* gene expression and blood pressure responses in SMC-specific *Tric-a*-transgenic mice.** (*A*) Changes in body weight of the *Tric-a*-transgenic mice and wild-type littermates. No significant difference was observed between the genotypes. (*B*) RT-PCR detection of *Tric-a* mRNA derived from the endogenous gene (EG) and the transgene (TG). Total tissue RNA preparations from at least three mice of each genotype were examined by quantitative RT-PCR analysis, and amplified cDNAs were analyzed on agarose gel electrophoresis. Expression of *Tric-b* mRNA was also examined in parallel (data not shown). (*C*) Relative expression of *Tric-a* and *Tric-b* mRNAs in tissues from the *Tric-a*-transgenic mice. The cycle threshold (Ct) was determined from the cDNA amplification curve as an index for relative mRNA content in each reaction. (*D*) Normal TRIC-A protein levels in the heart and skeletal muscle from the *Tric-a*-transgenic mice. Postnuclear lysates (2 and 0.5 μg protein for heart and skeletal muscle, respectively) from the *Tric-a*-transgenic, *Tric-a*-knockout and wild-type mice were analyzed by Western blotting using an antibody against the TRIC-A protein. Although RT-PCR detected transgene expression in striated muscle, TRIC-A protein levels were not significantly elevated in the heart or skeletal muscle. (*E*) Pharmacological effects of various agents on systolic blood pressure monitored by tail-cuff plethysmography in the *Tric-a*-transgenic and wild-type mice during daylight hours. Drugs used for analysis were the α1-antagonist prazosin (Pra, 1 mg/kg), α2-agonist clonidine (Clo, 0.1 mg/kg), angiotensin II AT1-receptor blocker candesartan (Can, 10 mg/kg), Rho kinase inhibitor Y27632 (5 mg/kg), dihydropyridine Ca^{2+} antagonist nicardipine (Nic, 1 mg/kg), phenylalkylamine Ca^{2+} antagonist verapamil (Ver, 12 mg/kg), muscarinic antagonist atropine (Atr, 4 mg/kg) and β1-antagonist metoprolol (Met, 4 mg/kg). The effects of autonomic blockage with atropine and metoprolol were slightly time-dependent, and the data at approximately 5 min and 15-30 min after drug injection are presented. The data represent the mean ± SEM, and no significant difference was detected between the genotypes in each response.

SUPPLEMENTARY FIGURE S2. **Histological analysis of mesenteric arteries from SMC-specific *Tric-a*-transgenic mice.** (*A*) Normal histological parameters of mesenteric arteries from *Tric-a*-transgenic mice. After incubation in a Ca^{2+}-free solution, relaxed mesenteric arteries were fixed for anatomical analysis and observed with a photomicroscope. We analyzed the media diameter, lumen diameter, media thickness, media to lumen diameter and lumen cross-sectional area (LCSA) of the arterial sections from three mice using Image J software. No significant difference was detected between the genotypes in each analysis. (*B*) Immunocytochemical detection of TRIC-A protein in *Tric-a*-overexpressing VSMCs. *Tric-a*-overexpressing and wild-type VSMCs were immunostained using antibodies to TRIC-A protein and the ER marker calnexin and examined using a confocal microscope. No immunostaining with anti-TRIC-A antibody was detected in

wild-type VSMCs (upper row), but dense immunostaining was observed at perinuclear regions in *Tric-a*-overexpressing VSMCs from TgA3 mice (middle row). VSMC images using a differential interference contrast (DIC) microscope are also presented. Numbered inset regions are also shown at high magnification (lower row). Scale bars, 2 μm.

SUPPLEMENTARY FIGURE S3. **Signaling proteins, total K^+ currents and resting membrane potential in *Tric-a*-overexpressing VSMCs.** (*A*) Quantitative RT-PCR analysis in mesenteric artery (MA) and thoracic aorta. The cycle threshold (Ct) was determined from the cDNA amplification curve as an index for relative mRNA content. For the data presentation, the mRNAs examined are tentatively categorized into four groups. Statistical evaluation detected no significant differences between the genotypes. (*B*) Cell-surface K^+ channel density in VSMCs. Single VSMCs were examined using the BK pipette solution and depolarized from a holding potential of -60 mV to test potentials in 10 mV steps. Representative current traces before and after iberiotoxin (IBTX) application are shown. Currents evoked at test potentials were normalized to membrane capacitance to yield the current density, and the data obtained are summarized as current-voltage relationship curves in the right graph. We detected no altered IBTX-sensitive or IBTX-insensitive currents in *Tric-a*-overexpressing VSMCs. (*C*) Direct membrane potential recordings using high-resistance microelectrodes in VSMCs. The left panel shows representative recording traces from the *Tric-a*-transgenic (TgA20), *Tric-a*-knockout and wild-type VSMCs. The recording data from six TgA20 mice, five *Tric-a*-knockout and five wild-type mice are summarized in the right graph. The data represent the mean ± SEM, and the numbers of cells examined are shown in parentheses. Significant differences are indicated by asterisks (*****p<0.05, ******p<0.01 vs wild-type controls by *t*-test).

SUPPLEMENTARY FIGURE S4. **Altered intracellular Ca^{2+} stores in *Tric-a*-overexpressing VSMCs.** (*A*) Representative sequential responses to caffeine (Caf, 10 or 30 mM) and phenylephrine (PE, 100 μM) under Ca^{2+}-free conditions in VSMCs from the *Tric-a*-transgenic, *Tric-a*-knockout and wild-type mice. Peak amplitudes ($\Delta F_{340}/F_{380}$) represent the mean ± SEM. Significant differences between the mutant and wild-type VSMCs are indicated by asterisks (*****p<0.05, ******p<0.01 by *t*-test). ND, not detected. (*B*) Hypothetical scheme for TRIC-A channel-mediated regulation of Ca^{2+} spark generation in VSMCs. Although the ionic fluxes are largely unknown in intracellular stores, this over-simplified model for caffeine-sensitive stores assumes that only TRIC-A and RyR2 channels carry counter-K^+ currents coupled with Ca^{2+} sparks in VSMCs. The colored channels contribute to net ionic fluxes across the SR membrane. Additionally, two undetectable Ca^{2+} release processes are proposed during the growth to visualized Ca^{2+} sparks (lower row); initial Ca^{2+} release by incidental RyR opening primarily depends upon the Ca^{2+} gradient between the SR and the cytoplasm (upper row), whereas the subsequent signal amplification mediated by Ca^{2+}-induced Ca^{2+} release (CICR) is likely to

require counter-K^+ currents for neutralizing the membrane potential generated by Ca^{2+} release (middle row). *Tric-a*-knockout and *Tric-a*-overexpressing VSMCs displayed a decrease or an excess of Ca^{2+} sparks, respectively. The observations suggest that Ca^{2+} spark generation depends critically upon TRIC-A-mediated K^+ current density in the SR; K^+ currents are likely to stabilize the SR membrane potential and thus effectively maintain the CICR-mediated amplification for Ca^{2+} spark generation. Because RyR subtypes are poorly selective cation channels that can conduct K^+ and Ca^{2+} bidirectionally, they may be responsible for contributing to the overall counter-ion current. Presumably, any counter-ion current via RyRs becomes important for the Ca^{2+} sparks and caffeine-induced transients observed in *Tric-a*-knockout muscle cell types.

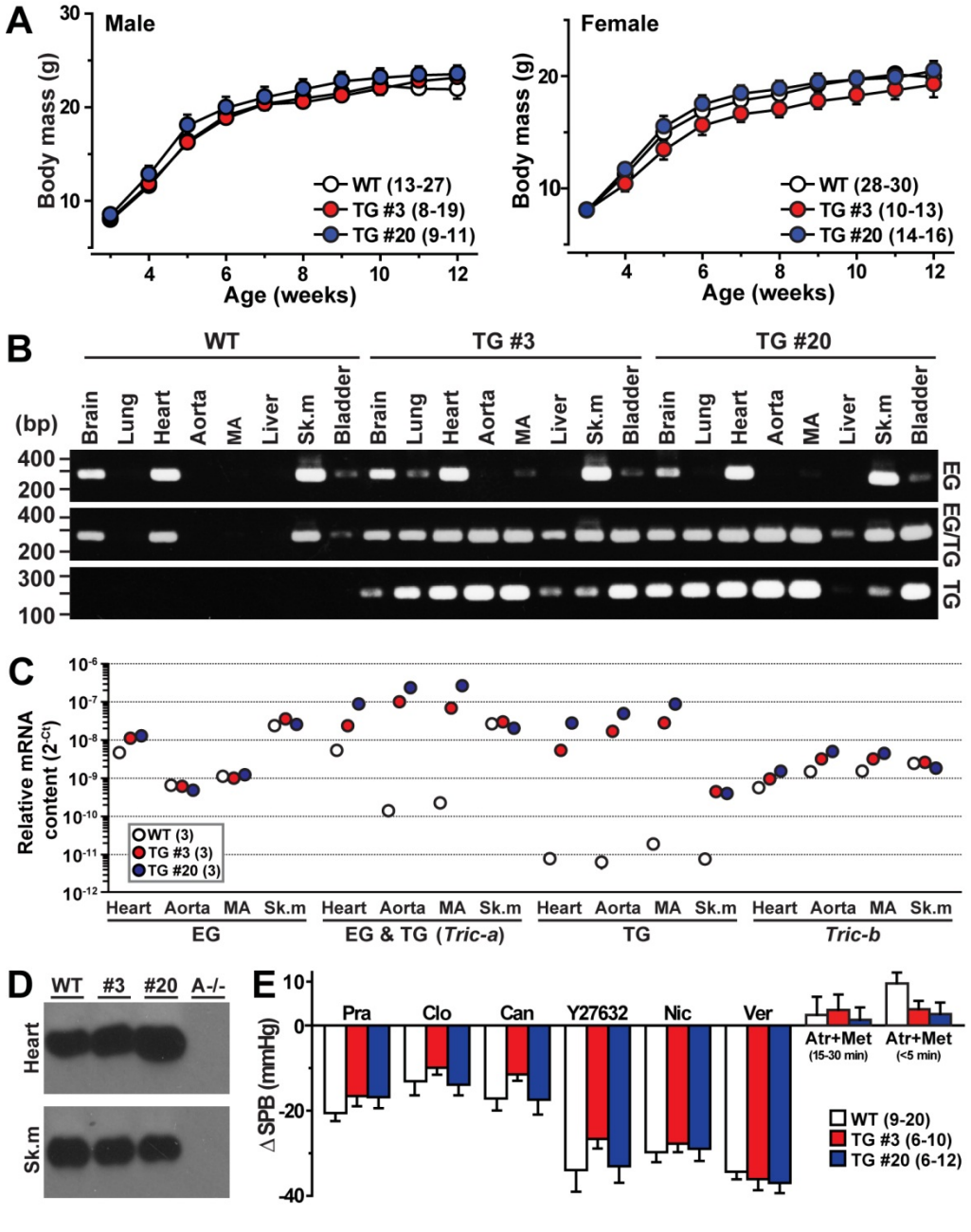
A
Male
Female
Body mass (g)
Age (weeks)
WT (13-27)
TG #3 (8-19)
TG #20 (9-11)
WT (28-30)
TG #3 (10-13)
TG #20 (14-16)
B
WT
TG #3
TG #20
Brain
Lung
Heart
Aorta
MA
Liver
Sk.m
Bladder
(bp)
EG
EG/TG
TG
C
Relative mRNA content (2-Ct)
WT (3)
TG #3 (3)
TG #20 (3)
EG
EG & TG (Tric-a)
TG
Tric-b
D
WT
#3
#20
A-/-
Heart
Sk.m
E
ΔSPB (mmHg)
Pra
Clo
Can
Y27632
Nic
Ver
Atr+Met (15-30 min)
Atr+Met (<5 min)
WT (9-20)
TG #3 (6-10)
TG #20 (6-12)

Figure S1

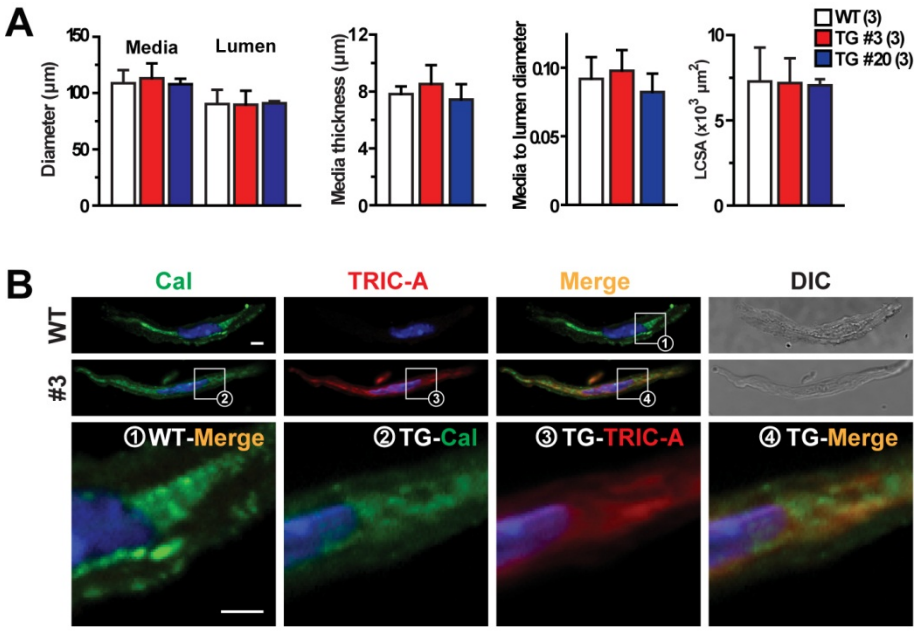
A
Media
Lumen
Diameter (μm)
150
100
50
0
Media thickness (μm)
12
8
4
0
Media to lumen diameter
0.10
0.05
0
LCSA (x10³ μm²)
10
5
0
WT (3)
TG #3 (3)
TG #20 (3)
B
Cal
TRIC-A
Merge
DIC
WT
#3
①WT-Merge
②TG-Cal
③TG-TRIC-A
④TG-Merge

Figure S2

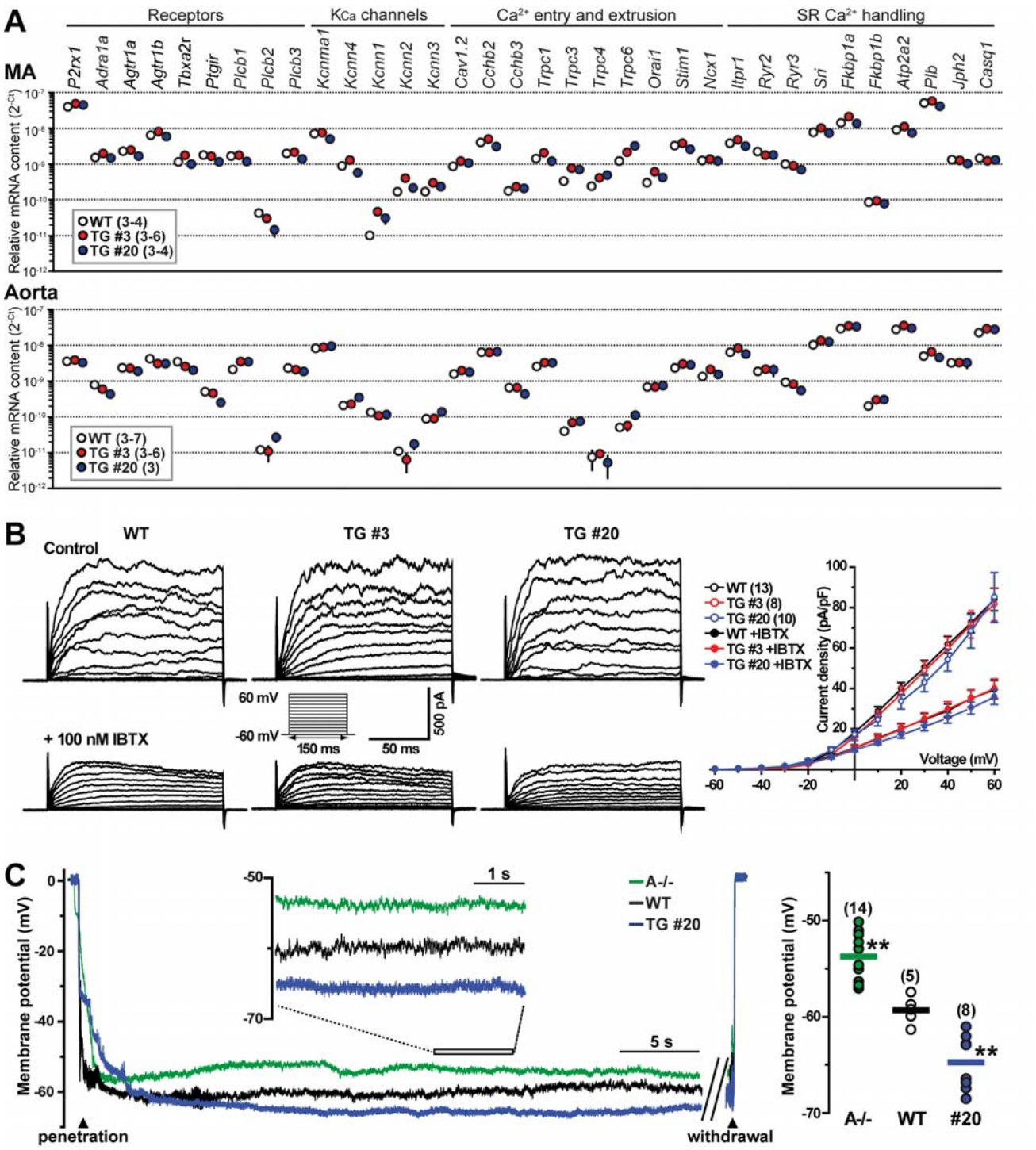
A
Receptors
KCa channels
Ca2+ entry and extrusion
SR Ca2+ handling
P2rx1
Adra1a
Agtr1a
Agtr1b
Tbxa2r
Ptgir
Plcb1
Plcb2
Plcb3
Kcnma1
Kcnn4
Kcnn1
Kcnn2
Kcnn3
Cav1.2
Cchb2
Cchb3
Trpc1
Trpc3
Trpc4
Trpc6
Orai1
Stim1
Ncx1
Itpr1
Ryr2
Ryr3
Sri
Fkbp1a
Fkbp1b
Atp2a2
Plb
Jph2
Casq1
MA
Relative mRNA content (2-Ct)
WT (3-4)
TG #3 (3-6)
TG #20 (3-4)
Aorta
WT (3-7)
TG #3 (3-6)
TG #20 (3)
B
WT
TG #3
TG #20
Control
+ 100 nM IBTX
60 mV
-60 mV
150 ms
50 ms
500 pA
WT (13)
TG #3 (8)
TG #20 (10)
WT +IBTX
TG #3 +IBTX
TG #20 +IBTX
Current density (pA/pF)
Voltage (mV)
C
Membrane potential (mV)
1 s
5 s
A-/-
WT
TG #20
penetration
withdrawal
(14)
(5)
(8)
**
**
A-/-
WT
#20

Figure S3

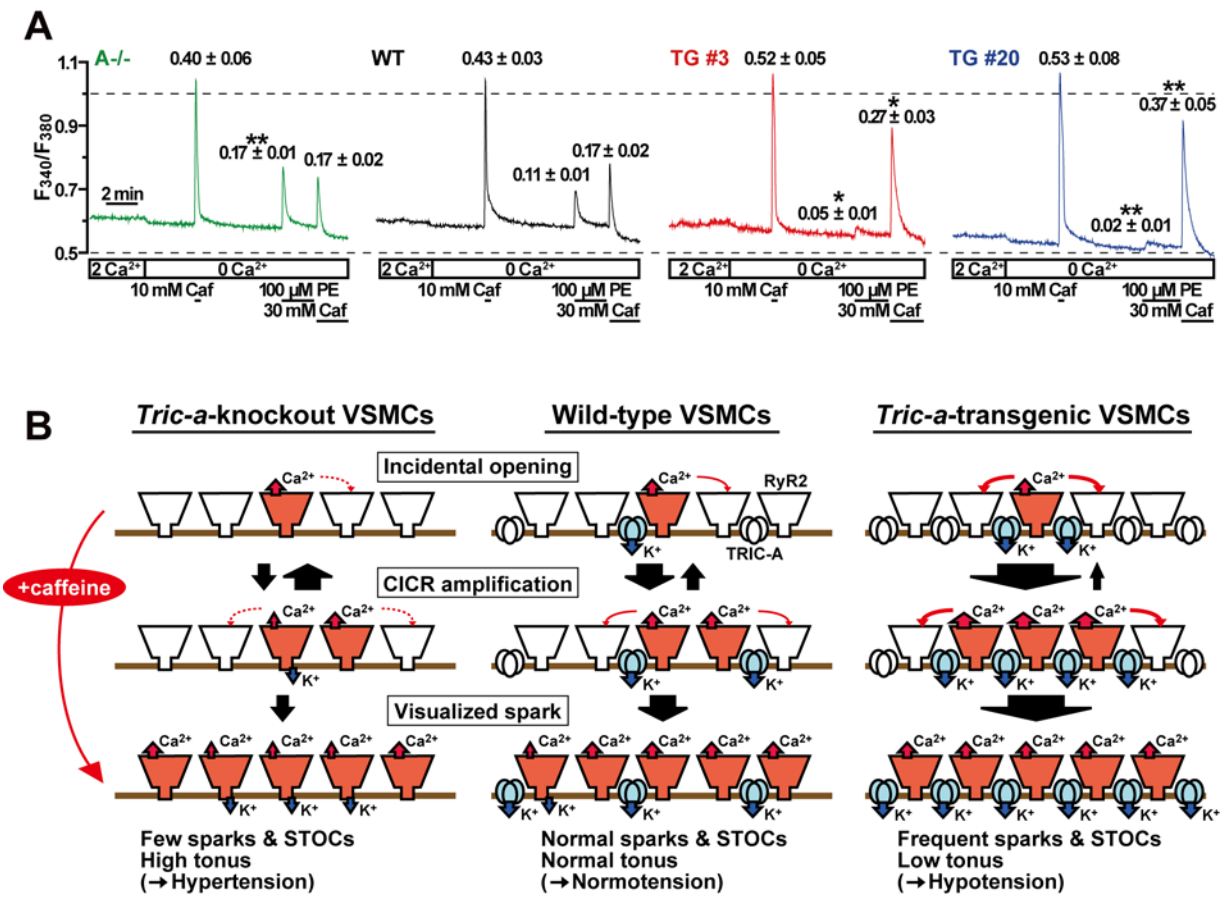
A
A-/-
0.40 ± 0.06
WT
0.43 ± 0.03
TG #3
0.52 ± 0.05
TG #20
0.53 ± 0.08
F340/F380
1.1
0.9
0.7
0.5
2 min
0.17 ± 0.01
0.17 ± 0.02
0.11 ± 0.01
0.17 ± 0.02
0.27 ± 0.03
0.05 ± 0.01
0.37 ± 0.05
0.02 ± 0.01
2 Ca2+
0 Ca2+
10 mM Caf
100 µM PE
30 mM Caf
B
Tric-a-knockout VSMCs
Wild-type VSMCs
Tric-a-transgenic VSMCs
Incidental opening
CICR amplification
Visualized spark
+caffeine
Ca2+
K+
RyR2
TRIC-A
Few sparks & STOCs
High tonus
(→Hypertension)
Normal sparks & STOCs
Normal tonus
(→Normotension)
Frequent sparks & STOCs
Low tonus
(→Hypotension)

Figure S4